Journal of Aerosol Science 100 (2016) 53–60

Contents lists available at ScienceDirect

Journal of Aerosol Science

journal homepage: www.elsevier.com/locate/jaerosci

Precision charging of microparticles in plasma via the Rayleigh instability for evaporating charged liquid droplets

E.D. Bennet [a], C.M.O. Mahony [c], H.E. Potts [a], P. Everest [b], D. Rutherford [c], S. Askari [c], D.A. McDowell [c], D. Mariotti [c], C. Kelsey [c], F. Perez-Martin [c], N. Hamilton [c], P. Maguire [c], D.A. Diver [a,*]

[a] SUPA, School of Physics and Astronomy, University of Glasgow, Glasgow G12 8QQ, United Kingdom
[b] Institute of Infection, Immunity and Inflammation, University of Glasgow, Glasgow G12 8TA, United Kingdom
[c] NIBEC, University of Ulster, Newtownabbey, Co Antrim BT37 0QB, United Kingdom

ARTICLE INFO

Article history:
Received 3 February 2016
Received in revised form
29 April 2016
Accepted 3 May 2016
Available online 11 May 2016

Keywords:
Charged droplets
Plasma
Instability
Target Charging
Electrostatics

ABSTRACT

In this paper we describe a novel method for delivering a precise, known amount of electric charge to a micron-sized solid target. Aerosolised microparticles passed through a plasma discharge will acquire significant electric charge. The fluid stability under evaporative stress is a key aspect that is core to the research. Initially stable charged aerosols subject to evaporation (i.e. a continually changing radius) may encounter the Rayleigh stability limit. This limit arises from the electrostatic and surface tension forces and determines the maximum charge a stable droplet can retain, as a function of radius. We demonstrate that even if the droplet charge is initially much less than the Rayleigh limit, the stability limit will be encountered as the droplet evaporates. The instability emission mechanism is strongly linked to the final charge deposited on the target, providing a mechanism that can be used to ensure a predictable charge deposit on a known encapsulated microparticle.

1. Introduction

This paper presents a theoretical calculation of evaporating charged water droplets, each of which contains a single solid micron-sized dust grain. By exploiting the Rayleigh instability of the droplets, the water can act as a moderator to deliver a known, final charge to any encapsulated solid target. The magnitude of charge deposited depends only on the terminal radius, and is independent of the initial conditions. It is important to have a better and fundamental understanding of liquid droplets that interact with a plasma environment where the possibility of not just precision charging of encapsulated particles but also interfacial plasma–liquid chemistry opens up many novel application areas.

The motivation for this is a multi-disciplinary collaborative investigation into aerosol transport through plasma, for which the ultimate goal is the development of a novel bacteria detector. Maguire et al. (2015) have experimentally demonstrated that aerosols can be passed through a microplasma. They report a decrease in droplet size beyond normal evaporation, and experiments are ongoing to determine the nature of these effects, and to obtain an accurate measurement

* Corresponding author.
E-mail address: declan.diver@glasgow.ac.uk (D.A. Diver).

http://dx.doi.org/10.1016/j.jaerosci.2016.05.002

of charge deposited by the plasma. Early measurements indicate agreement with theoretical predictions of 10^5 electrons per 3 μm-radius droplet (Maguire, 2016).

A 4-stage charging process has been identified:

1. The target (i.e. the grain) is aerosolised and becomes encapsulated in a water droplet, and so is significantly larger as a charging target than its dry radius.
2. The droplets are exposed to a plasma and acquire a stable charge, well below the Rayleigh limit for that radius.
3. There is forced evaporation of the droplet, both in and out of the plasma, such that the Rayleigh limit is encountered as the radius decreases.
4. The charge tracks the Rayleigh limit until the target is exposed, whereupon the charge acquired by the target is known to greater precision than that on the original droplet.

There are many diverse examples to be found in the literature of both experimental and theoretical studies of charged liquid droplets (delaMora, 1996; Doyle, Moffett, & Vonnegut, 1964; Feng, Bogan, & Agnes, 2001; Hunter & Ray, 2009; Taflin, Ward, & Davis, 1989; Thaokar & Deshmukh, 2010; Widmann, Aardahl, & Davis, 1997). The theory of their behaviour dates back to Rayleigh's work in 1882 (Lord Rayleigh, 1882) where he demonstrated that electrically charged liquid droplets will remain stable given any perturbation as long as their total charge is less than the limit

$$Q_R = 8\pi\sqrt{\varepsilon_0 \gamma r_d^3} \tag{1}$$

where ε_0 is the permittivity of free space, γ is the surface tension of the liquid, and r_d is the radius of the droplet. If the charge on the droplet $Q_d > Q_R$ then electrostatic repulsion can overcome the surface tension, and some mass and charge is emitted via a Taylor cone (Taylor, 1964).

The dynamics of charged droplets formed by electrosprays have also been extensively studied (Daly, Kerby, & Austin, 2013; Hogan, Biswas, & Chen, 2009; Maze, Jones, & Jarrold, 2006; Seto et al., 2013; Zilch, Maze, Smith, Ewing, & Jarrold, 2008). In particular, Zilch et al. (2008) found that charged droplets produced by several experimental techniques were quite uniform in size and charge. In Seto et al. (2013) it was shown that some particular sizes of electric charge in a water cluster are more stable than others. The consensus appears to be that if water droplets are charged, then normal evaporation will occur until near the Rayleigh limit, at which point the charge on the evaporating droplet will track the maximum provided by that limit.

It has been demonstrated experimentally (Davis & Bridges, 1994; Gomez & Tang, 1994; Hogan et al., 2009; Li, Tu, & Ray, 2005; Seto et al., 2013; Smith, Flagan, & Beauchamp, 2002) that charged droplets will expel clusters of charged molecules while near the theoretical Rayleigh limit. Gomez and Tang (1994) report photographs of droplets undergoing the expulsion of much smaller droplets. The smaller ejected droplets must be stable (i.e. below the Rayleigh limit) in their own right, and proceed to evaporate as normal for their size. In emitting via this mechanism (fine fission) the larger droplet can remain stable and evaporate continuously, without suffering a catastrophic Coulomb explosion in which the daughter droplet masses are a significant proportion of the parent droplet mass (rough fission) (delaMora, 1996).

This paper is structured as follows: the next section addresses how a droplet in a plasma acquires significant free charge; Section 3 discusses how that acquired free charge induces the Rayleigh instability as the drop evaporates; Section 4 then models the process holistically, to show how a typical droplet undergoes several charge-loss events to end up with a final charge, at its terminal radius, that depends on the history of these events. A concluding discussion reviews the process and its technological application to the precision charging of droplet-encased particulates.

2. Theoretical model of droplets in plasma

Wherever a surface is introduced to an electrical discharge, it is subjected to a flux of positive and negative species from the plasma. However, because the electrons in the plasma are very much more mobile than any other species (being much lighter than protons, and therefore moving much faster for a given kinetic energy), there are initially more electron encounters with the surface than is the case for the positive ions. As a consequence, the surface acquires a significant negative charge, repelling less energetic electrons and attracting positive ions. The surface continues to charge negatively until a balance is reached, in which the fluxes of positive and negative species are equal – this process takes only nano-seconds to complete. By this stage the surface is now a negative equipotential (the plasma potential), and surrounded by a region in which the electron population is depleted relative to the rest of the plasma (by virtue of the repulsive potential), but the positive ion population is accelerated: such a region is termed the sheath, and is typically a few Debye lengths in extent. In this paper, the surfaces of interest are those of the discrete aerosols introduced to the discharge region.

Droplets entering plasma undergo the normal charging process for a surface immersed in a discharge: a sheath forms between the droplet surface and the plasma, and the electron and ion currents to the surface reach equilibrium when the droplet is at the plasma potential. Consider the solid targets to be spheres of radius $r_b \approx 1$ μm, each within spherical water droplets of radius $r_d = 10$ μm.

When immersed in plasma, the rate of charging $\dot{Q}$ of the droplet is given by the sum of the electron I_e and ion I_i currents:

$$\dot{Q} = I_e + I_i \tag{2}$$

and the potential on the surface with respect to the field point at infinity can be written in terms of the charge on the droplet:

$$\phi = \frac{Q}{4\pi\epsilon_0 r_d} \tag{3}$$

This dynamic equilibrium is sustained by the balanced electron and ion currents for as long as the droplet is inside the plasma. When the droplet leaves the plasma it retains whatever surface charge was deposited on it, because although the free charge in the plasma is confined by the electromagnetic fields that sustain it, the aerosol has more than enough momentum to escape the plasma region, and take with it the trapped charge on its surface.

The sheath between the plasma and any surface can be considered to be collisionless if the mean free path of ions l_i is greater than the sheath length λ_S. Under these conditions the orbital motion limited (OML) model for a charging a small spherical surface in the plasma is a reasonable approximation (Lieberman & Lichtenberg, 2005). However, if $l_i < \lambda_S$ then on average ions will collide with one or more neutral atoms while crossing the sheath, and the plasma sheath must be considered to be collisional. It is well known that the OML approximation for ion current no longer holds in such circumstances (Khrapak et al., 2005; Lampe, Gavrishchaka, Ganguli, & Joyce, 2001; Zobnin, Nefedov, Sinel'Shchikov, & Fortov, 2000). Several refined models of ion current have been developed to account for ion collisionality (Khrapak & Morfill, 2008; Patacchini & Hutchinson, 2009), depending mainly on plasma conditions such as relative Debye length. Regimes featuring larger, even macroscopic, dust grains ($r_d \gg \lambda_D$) have been modelled empirically (Hutchinson & Patacchini, 2007) and measured experimentally (Khrapak et al., 2012).

The electron and ion currents together with Eq. (3) define the evolution of charge on the droplet whilst it is in the plasma. The appropriate charging timescale is of order nanoseconds across the models – far more rapid than any other physically relevant timescale. The charge deposited on the droplet is defined by the establishment of a dynamic equilibrium that balances the electron and ion currents for as long as the droplet is inside the plasma; upon leaving the plasma environment, the droplet retains that deposited surface charge. Both collisional ion current models explored here (Khrapak & Morfill, 2008; Patacchini & Hutchinson, 2009) agree on the value of the final charge to within a factor of two; indeed this is evident in Fig. 10 of Patacchini and Hutchinson (2009).

Since the main thesis of this paper is that the behaviour of the evaporating droplet will control the charge evolution irrespective of its starting value, as long as there is sufficient initial charge to ensure at least one Rayleigh instability is encountered during the evaporation stage, then specifying the initial charge precisely is less significant. Indeed, the modelling in this paper details a technique that compensates for the range of underlying uncertainty in the initial charging processes, from variability in the droplet size, uncertainty in the trajectory through the plasma region (which itself may be inhomogeneous) and collisional-sheath dynamics. Hence we may assume that the currents in the collisional case are given by (Khrapak & Morfill, 2008):

$$I_e = -I_{e0} \exp\left[e\phi/(k_B T_e)\right] \tag{4}$$

$$I_i = \left[\frac{1}{I_i^{WC}} + \frac{1}{I_i^{SC}}\right]^{-1} \tag{5}$$

where ϕ is the potential at the surface of the drop, and T_e is the electron temperature. The electron current term I_{e0} is (assuming a radial flux from the plasma to the droplet)

$$I_{e0} = \frac{1}{4} e n_e \bar{v}_e 4\pi r_d^2 \tag{6}$$

where n_e is the electron number density. The mean speed v_e is defined in terms of the electron temperature T_e and electron mass m_e:

$$\bar{v}_e = \left(\frac{8 k_B T_e}{\pi m_e}\right)^{1/2} \tag{7}$$

The ion current terms I_i^{WC} and I_i^{SC} are respectively the weakly collisional and strongly collisional correction terms:

$$I_i^{WC} = I_{i0}\left[1 - \frac{e\phi}{k_B T_i} + 0.1\frac{\lambda_D}{l_i}\left(\frac{e\phi}{k_B T_i}\right)^2\right] \tag{8}$$

$$I_i^{SC} = 4 I_{i0} \frac{l_i}{r_d} \frac{e|\phi|}{k_B T_i} \tag{9}$$

where T_i is the ion temperature, and I_{i0} is defined in the same form as I_{e0}, only with ion parameters instead of electron parameters.

Equations (4) and (5) together with Eq. (3) define the evolution of charge on the droplet whilst it is in the plasma.

The equilibrium potential (the plasma potential) is then given by the potential which balances the ion and electron currents, and is clearly a function of the plasma parameters and the drop size.

It has been reported (Shi & Blandino, 2013) that electron bombardment can control the mean size of a droplet distribution by forcing droplets to exceeding the Rayleigh charge limit. Our technique is different, but similar in underlying philosophy: rather than manipulating the charge to force droplet fission, we allow the plasma to decide the initial charge, but use evaporation to reduce the droplet radius, and so cause the Rayleigh instability to occur after the plasma charging process has ceased. In this way, we can control the final charge on an evaporated droplet.

3. Harnessing the Rayleigh instability to control grain charging

Evaporation determines the rate at which droplet mass is lost, and hence rate at which the droplet radius is reduced. Whilst inside the plasma, the particle currents to the surface of the droplet maintain the latter's surface potential at the plasma potential. Therefore the charge on the droplet is subject to the dynamic equilibrium of the plasma potential (Eqs. (2) and (3)).

As the droplet radius shrinks by evaporation, the balance of electron and ion currents changes. To maintain the same plasma potential at the droplet surface as the radius reduces requires less net charge on the droplet, and hence evaporation inside the plasma forces the droplet charge to reduce.

Once outside the plasma discharge region, the charged particle currents to the droplet surface cease and the droplet retains the final charge deposited by the plasma. Let the droplet charge on exit be $Q_0 = \alpha Q_{R0}, \alpha < 1$, so that the exit droplet charge is less than its exit Rayleigh limit charge Q_{R0} and therefore it is stable. As the droplet evaporates in neutral gas, the charge on it remains approximately constant as long as the Rayleigh stability conditions are met.

However, as the droplet radius drops, so too does the Rayleigh stability limit on the charge that it can carry. For an evaporating droplet with time-dependent radius $r(t)$, the evolving Rayleigh limit normalised to the initial stability limit of the droplet can be expressed in the quantity $\beta(t)$, where

$$\beta(t) = \frac{Q_R(t)}{Q_{R0}} = \left[\frac{r(t)}{r_0}\right]^{3/2} \tag{10}$$

in which $r_0 = r(t=0)$ is the initial value of the droplet radius. Even if the initial droplet charge is much less than the Rayleigh limit, the reduction with time of the latter will may allow the instability can be exploited some time after the initial charge is delivered. If $Q_R(t)$ decreases far enough that $Q_R(t) \approx Q$, then the droplet will become unstable and emit sufficient charge to endure that the new charge Q' restores the stability condition of $Q' < Q_R(t)$. Evaporation then continues as normal, until once again the stability condition is broken and more charge is emitted. This feedback loop continues until the droplet evaporation ceases.

If evaporation cannot proceed beyond a minimum radius r_m, for example to account for a microscopic target inside the droplet, then the final charge on the droplet at $t = t_f$ can be found by combining Eqs. (1) and (10):

$$\begin{aligned} Q(t_f) &\approx \beta(t_f) Q_{R0} = Q_R(t_f) \\ &\approx 8\pi\sqrt{\gamma \varepsilon_0 r_m^3} \end{aligned} \tag{11}$$

The upper limit of final droplet charge depends only on the minimum radius of the particle left behind once the droplet has evaporated, irrespective of the initial charge. This holds provided that the Rayleigh limit is encountered at some intermediate point in the evaporative evolution of the drop.

The model presented describes droplets consisting of pure water, with surface tension γ. If the droplets instead consisted of an electrolytic solution (such as those used in e.g. Wang, Tan, Go, & Chang, 2012; Zardini, Riipinen, Koponen, Kulmala, & Bilde, 2010) then they would have a modified surface tension $\gamma' < \gamma$ which would enter Eq. (1). This would ultimately mean that the Rayleigh instability is first encountered earlier during evaporation than it would be in pure water. According to Eq. (11) the final charge deposited on the dust grain would also be reduced by a factor $\sqrt{\frac{\gamma'}{\gamma}}$.

Note that the surface tension can also be affected by an externally applied voltage, where the latter is in the kV range (Santos, Ducati, Balestrin, & Galembeck, 2011). Since the plasma potential useful for the practical application of this technique would be of order < 10 V this influence will not be important here.

Note also that the dielectric nature of the droplet liquid might influence the Rayleigh limiting charge, reducing it below the classical limit by a factor that depends on the relative dielectric permittivity (Shrimpton, 2005). Hence dielectric droplets may actually become unstable to fission at smaller charge values.

4. Results

A numerical solution by finite difference was written to solve for the charge evolution of droplets containing solid targets. Droplets are carried by atmospheric-pressure gas flow through a narrow plasma discharge region and go on to evaporate in neutral gas, leaving a charged dust grain surrounded by little or no water. Following Cazabat and Guena (2010),

during atmospheric evaporation the surface area of the droplet reduces linearly with time; this assumption (rather than a full kinetic description of evaporation Chernyak, 1995) allowed the time evolution of the simulations to be scaled to the time taken for complete droplet evaporation. The dynamic equilibrium of droplets evaporating in a collisional plasma was carefully taken into account, since a significant fraction of evaporation time may be spent in the plasma. Figure 1 shows the radius and charge evolution of an average droplet.

Simulations were carried out for six populations, each of 1000 targets. Each population has a different mean radius. After the simulated charging in the plasma and subsequent droplet evaporation, the final charge-to-mass ratio of the targets was

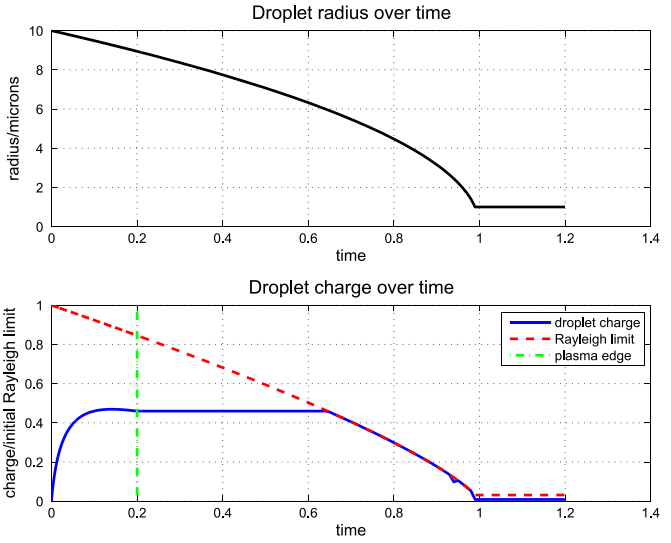

Fig. 1. Shown in this figure is the case of a typical droplet which might spend about 20% of its lifetime in the plasma. The top plot shows the radius evolution as the droplet evaporates. Depicted in the bottom plot are the charge (solid blue line) and Rayleigh limit (dashed red line) of an evaporating water droplet containing a dust grain that is one-tenth of the initial droplet radius. Time is normalised to the time taken for the water droplet to completely evaporate, leaving the target. The droplet enters the plasma at $t=0$ and charges very rapidly. While still in the plasma (left of the vertical dot-dashed green line) the plasma potential is imposed at the droplet surface. Outside the plasma the droplet evaporates as normal in neutral gas. The charge on the droplet remains relatively constant until the stability limit is reached, at which point the droplet emits enough charge to remain stable and enters a feedback cycle of emission and evaporation. The final charge deposited on the target is closely linked to the Rayleigh limit of the minimally-encapsulating droplet. (For interpretation of the references to colour in this figure caption, the reader is referred to the web version of this paper.)

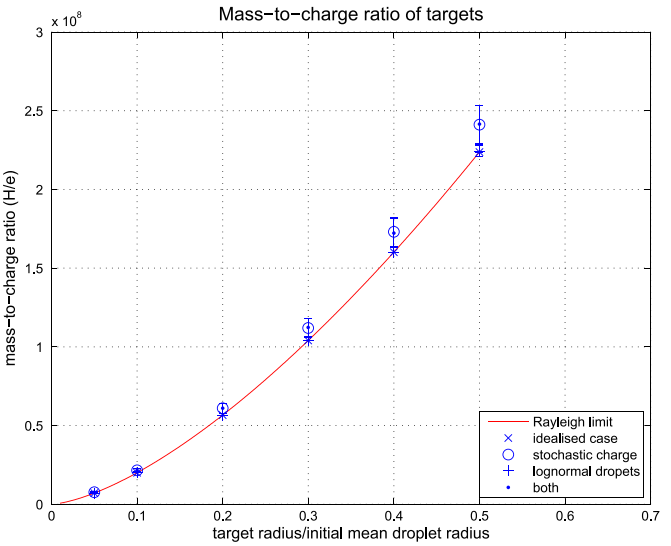

Fig. 2. The mean mass-to-charge ratio of each of the six populations of targets. Error bars denote the standard deviation of each population. The source of uncertainty in the cases with stochastic charge emission arises because different amounts of charge are emitted in the 'final' instability event. The red line shows the theoretical Rayleigh limit for the target radius, scaled by target mass. Notice that the mass-to-charge ratio of the targets on average corresponds very closely to the Rayleigh limit, as was predicted theoretically. (For interpretation of the references to colour in this figure caption, the reader is referred to the web version of this paper.)

calculated: the mass-to-charge ratio (m/z) expresses, in convenient units, the quotient of the target mass (in multiples of unified amu or daltons, that is, one twelfth the mass of Carbon 12) and the target charge (in units of the number of electrons) (Da/e); unity in this convenient unit is equivalent to 1.04×10^{-8} kg/C, in SI units. In practice, for example in mass spectrometry, mass-to-charge ratio will be the primary observable for experimental purposes.

To establish which mechanisms could introduce uncertainty to our proposed technique, eight theoretical cases in total were considered. The first four cases described below focus on the uncertainties introduced by the initial droplet population and by the mechanism for charge emission during instability events.

1. The idealised case in which the initial droplet population is a Dirac delta-function, and the charge emission mechanism is quantised: each instability event causes the emission of progeny nano-droplets each carrying an identical charge. Hence the charge lost by the parent droplet is simply the product of the number of progeny and the charge quantum. This charge emission model is similar to that described in Gu, Heil, Choi, and Kim (2007) and Hunter and Ray (2009).
2. The initial droplet population is a Dirac delta-function, but charge emission is handled stochastically, with the droplet emitting a random amount of charge during each instability event – up to 20% of the extant total. Charge emission has been reported to appear stochastic in experiments (Doyle et al., 1964; Gomez & Tang, 1994).
3. The initial droplet population is a lognormal distribution, rather than a Dirac delta-function. Charge emission is quantised, as described in case 1.
4. The initial droplet population is a lognormal distribution, while charge emission is stochastic, as in case 2.

The results of these four cases are plotted in Fig. 2. Final charge deposited corresponds closely to the theoretical Rayleigh limit. An uncertainty in final charge deposited is introduced in the two stochastic cases, and relates to the uncertainty in charge emitted during the final instability event before evaporation is completed. For the target radii shown in Fig. 2, targets of each size would be clearly distinguishable for the purposes of experimental detection, in terms of their mass-to-charge ratio.

In order to assess the impact of non-uniform target distributions on the final charge on an evaporated droplet, additional four cases were modelled. The significance of variation in the target radius is that it influences the terminal evaporation radius, and hence the number of charge emission events in the lifetime of a charged droplet.

5. The idealised case: The initial droplet distributions are again Dirac delta-functions, and the target is a single exact radius. The scenario here is essentially the same as in case 1 above.
6. The initial droplet population is a delta-function. Target distributions are Gaussian, with a variance in radius of 20%.
7. The initial droplet population is a lognormal distribution. Target distributions are uniform, as described in case 5.
8. The initial droplet population is a lognormal distribution, while target distributions are Gaussian, as in case 6.

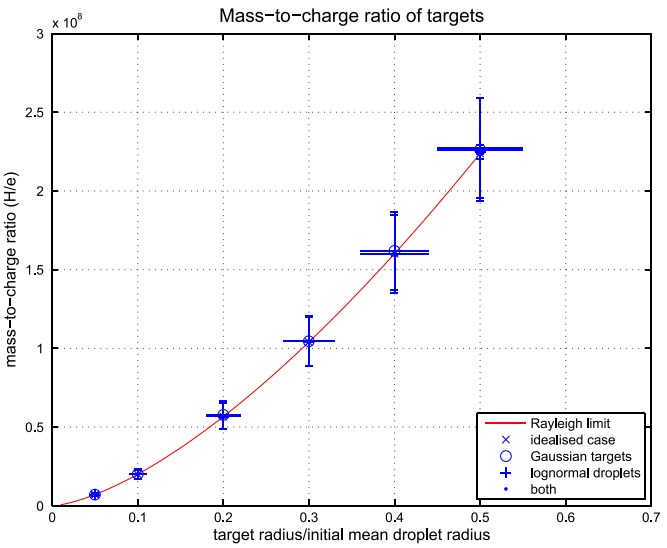

Fig. 3. The mean mass-to-charge ratio of each of the six populations of targets. Error bars denote the standard deviation of each population. In these cases a source of uncertainty in the x-direction is introduced by the spread in target radius, but is *not* introduced by a spread in droplet radius. The red line shows the theoretical Rayleigh limit for the target radius, scaled by target mass. Notice that the mass-to-charge ratio of the targets on average corresponds very closely to the Rayleigh limit, as was predicted theoretically. Additionally, targets with different radii would be experimentally distinguishable, in the sense that the uncertainty ranges of the final mass-to-charge ratios do not overlap. (For interpretation of the references to colour in this figure caption, the reader is referred to the web version of this paper.)

Table 1
An example of how targets between 0.5 μm and 5 μm in radius can be sorted by mass-to-charge ratio. The uncertainties show the standard deviation. For each set of target radii, the mass-to-charge ratio is unique and does not overlap with any other set.

Target radius (dimensionless)	Target radius (microns)	Charge delivered (electrons)	Mass-to-charge ratio (Da/e)
0.05	0.5	$(4.5 \pm 0.7) \times 10^4$	$(7 \pm 1) \times 10^6$
0.1	1	$(1.3 \pm 0.2) \times 10^5$	$(2.0 \pm 0.3) \times 10^7$
0.2	2	$(3.6 \pm 0.5) \times 10^5$	$(5.7 \pm 0.8) \times 10^7$
0.3	3	$(6.5 \pm 0.9) \times 10^5$	$(1.0 \pm 0.2) \times 10^8$
0.4	4	$(1.0 \pm 0.1) \times 10^6$	$(1.6 \pm 0.2) \times 10^8$
0.5	5	$(1.4 \pm 0.2) \times 10^6$	$(2.3 \pm 0.3) \times 10^8$

The results of these four cases are plotted in Fig. 3. Once again, smaller targets with higher charge-to-mass ratio would be clearly distinguishable experimentally. The charge deposited on the targets corresponds closely to the theoretical Rayleigh limit. The uncertainty introduced in the two cases where Gaussian populations of targets were modelled reflects the spread in the target radii which in turn alters the Rayleigh limit of the minimally-encapsulating droplet.

5. Discussion

This paper has proposed a theoretical model of a mechanism for depositing a known amount of electric charge onto micron-sized particulates that are encapsulated in water droplets. Using the encapsulating water droplet as a moderator for the acquired charge, the aerosolised targets can be reliably differentiated by size. By exploiting the Rayleigh instability, the final charge deposited depends only on the terminal radius of the target grain. We have demonstrated theoretically that this holds independent of charge emission mechanism and of the initial droplet distribution: as long as at least one Rayleigh instability is encountered during evaporation, a predictable magnitude of charge should be deposited. The distinguishable range of target sizes extends for an order of magnitude – i.e. the mass-to-charge ratio of targets over that range in radii is measurably unique. All target radii show statistically distinguishable mass-to-charge ratios. For larger radii, the experimental challenge to distinguish between different targets is greater than for targets of smaller radii. This could be mitigated by altering the plasma conditions.

We propose that the technique of using droplet evaporation as a moderator for charge deposition could provide a precise method for delivering a known amount of charge to microscopic particles. This mechanism offers precision beyond that of high-resolution mass spectrometry, with the additional advantage of being non-destructive to targets. It has the potential to be applied to directly study the electromechanical properties of targets such as bacteria cells. In high-precision mass spectrometry the m/z is small compared to m/z values here (of order 10^5 compared to 10^8).

Table 1 illustrates the potential of this proposed technique for sorting micron-sized targets by charge deposited.

One possible mechanism to enable further insight into the electromechanical properties of micron-size targets is to use an electrostatic trap to capture targets that have been charged using the method presented here. By utilising this method which deposits a precise amount of charge related to the size of the target, the electrostatic trap can be designed to specification. For example, smaller targets would have higher mass-to-charge ratio, and therefore for fixed trap electric field smaller targets would be stopped after less time than larger targets.

Preliminary experiments are underway, with initial findings that after passing through plasma, a rapid reduction in observed droplet size implies enhanced evaporation, possibly related to charge and surface chemistry effects. These results, along with a detailed experimental description, are presented in Maguire et al. (2015).

Acknowledgements

The authors gratefully acknowledge support from EPSRC via Grant numbers EP/K006142/1 and EP/K006088/1. We would like to acknowledge the initiative of the COST Action TD1208, which have contributed to significant knowledge exchange on the subject. Thanks are due also to the anonymous referees, whose careful observations have improved the paper. Lastly, we are grateful to Alasdair Wilson for his assistance in the preparation of this manuscript.

References

Cazabat, Anne-Marie, & Guena, Geoffroy (2010). Evaporation of macroscopic sessile droplets. *Soft Matter*, *6*(12), 2591–2612.
Chernyak, V. (1995). The kinetic-theory of droplet evaporation. *Journal of Aerosol Science*, *26*(September (6)), 873–885.
Daly, R. T., Kerby, J. D., & Austin, D. E. (2013). Electrospray charging of minerals and ices for hypervelocity impact research. *Planetary and Space Science*, *75* (January), 182–187.
Davis, E. J., & Bridges, M. A. (1994). The Rayleigh limit of charge revisited—light-scattering from exploding droplets. *Journal of Aerosol Science*, *25*(September (6)), 1179–1199.

delaMora, J. F. (1996). On the outcome of the Coulombic fission of a charged isolated drop. *Journal of Colloid and Interface Science*, *178*(1), 209–218.
Doyle, A., Moffett, D. R., & Vonnegut, B. (1964). Behaviour of evaporating electrically charged droplets. *Journal of Colloid Science*, *19*(2), 136–143.
Feng, X., Bogan, M. J., & Agnes, G. R. (2001). Coulomb fission event resolved progeny droplet production from isolated evaporating methanol droplets. *Analytical Chemistry*, *73*(September (18)), 4499–4507.
Gomez, A., & Tang, K. Q. (1994). Charge and fission of droplets in electrostatic sprays. *Physics of Fluids*, *6*(January (1)), 404–414.
Gu, W., Heil, P. E., Choi, H., & Kim, K. (2007). Comprehensive model for fine Coulomb fission of liquid droplets charged to rayleigh limit. *Applied Physics Letters*, *91*(August (6)), 064104.
Hogan, C. J., Jr., Biswas, P., & Chen, D. (2009). Charged droplet dynamics in the submicrometer size range. *Journal of Physical Chemistry B*, *113*(January (4)), 970–976.
Hunter, H. C., & Ray, A. K. (2009). On progeny droplets emitted during Coulombic fission of charged microdrops. *Physical Chemistry*, *11*(29), 6156–6165.
Hutchinson, I. H., & Patacchini, L. (2007). Computation of the effect of neutral collisions on ion current to a floating sphere in a stationary plasma. *Physics of Plasmas*, *14*(January (1)).
Khrapak, S. A., & Morfill, G. E. (2008). An interpolation formula for the ion flux to a small particle in collisional plasmas. *Physics of Plasmas*, *15*(November (11)), 114503.
Khrapak, S. A., Ratynskaia, S. V., Zobnin, A. V., Usachev, A. D., Yaroshenko, V. V., Thoma, M. H., et al. (2005). Particle charge in the bulk of gas discharges. *Physical Review E*, *72*(July (1)), 016406.
Khrapak, S. A., Tolias, P., Ratynskaia, S., Chaudhuri, M., Zobnin, A., Usachev, A., et al. (2012). Grain charging in an intermediately collisional plasma. *Europhysics Letters*, *97*(February (3)).
Lampe, M., Gavrishchaka, V., Ganguli, G., & Joyce, G. (2001). Effect of trapped ions on shielding of a charged spherical object in a plasma. *Physical Review Letters*, *86*(June), 5278–5281.
Li, K. Y., Tu, H. H., & Ray, A. K. (2005). Charge limits on droplets during evaporation. *Langmuir*, *21*(April (9)), 3786–3794.
Lieberman, M.A., & Lichtenberg, A.J. (2005). *Principles of plasma discharges and materials processing* (pp. 1–757), 2nd Edition.
Lord Rayleigh, J. W. S. (1882). On the equilibrium of liquid conducting masses charged with electricity. *Philosophical Magazine Series 5*, 14(87), 184–186.
Maguire, P. D., Mahony, C. M. O., Kelsey, C. P., Bingham, A. J., Montgomery, E. P., Bennet, E. D., et al. (2015). Controlled microdroplet transport in an atmospheric pressure microplasma. *Applied Physics Letters*, *106*(June (22)).
Maguire, P. D. (2016). Private communication.
Maze, J. T., Jones, T. C., & Jarrold, M. F. (2006). Negative droplets from positive electrospray. *Journal of Physical Chemistry A*, *110*(November (46)), 12607–12612.
Patacchini, Leonardo, & Hutchinson, Ian H. (2009). Continuum-plasma solution surrounding nonemitting spherical bodies. *Physics of Plasmas*, *16*(January (6)).
Santos, Leandra P., Ducati, Telma R. D., Balestrin, Lia B. S., & Galembeck, Fernando (2011). Water with excess electric charge. *Journal of Physical Chemistry C*, *115*(June (22)), 11226–11232 JUN 9.
Seto, T., Maekawa, T., Osone, S., Kawamura, K., Yamauchi, T., & Otani, Y. (2013). Formation of highly charged nanodroplets by condensation-electrospray device. *Chemical Engineering Science*, *85*(January), 46–49.
Shi, X., & Blandino, J. (2013). Effect of electron bombardment on size distribution of negatively charged droplets produced by electrospray. *Journal of Aerosol Science*, *59*(May), 31–46.
Shrimpton, J. S. (2005). Dielectric charged drop break-up at sub-Rayleigh limit conditions. *IEEE Transactions on Dielectrics and Electrical Insulation*, *12*(January (3)), 573–578.
Smith, J. N., Flagan, R. C., & Beauchamp, J. L. (2002). Droplet evaporation and discharge dynamics in electrospray ionization. *Journal of Physical Chemistry A*, *106*(October (42)), 9957–9967.
Taflin, D. C., Ward, T. L., & Davis, E. J. (1989). Electrified droplet fission and the rayleigh limit. *Langmuir*, *5*(March (2)), 376–384.
Taylor, G. (1964). Disintegration of water drops in electric field. *Proceedings of the Royal Society of London Series A—Mathematical and Physical Sciences*, 280 (1380), 383–397.
Thaokar, R. M., & Deshmukh, S. D. (2010). Rayleigh instability of charged drops and vesicles in the presence of counterions. *Physics of Fluids*, *22*(March (3)), 034107.
Wang, Yunshan, Tan, Ming K., Go, David B., & Chang, Hsueh-Chia (2012). Electrospray cone-jet breakup and droplet production for electrolyte solutions. *Europhysics Letters*, *99*(September (6)).
Widmann, J. F., Aardahl, C. L., & Davis, E. J. (1997). Observations of non-Rayleigh limit explosions of electrodynamically levitated microdroplets. *Aerosol Science and Technology*, *27*(November (5)), 636–648.
Zardini, A. A., Riipinen, I., Koponen, I. K., Kulmala, M., & Bilde, M. (2010). Evaporation of ternary inorganic/organic aqueous droplets: Sodium chloride, succinic acid and water. *Journal of Aerosol Science*, *41*(August (8)), 760–770.
Zilch, L. W., Maze, J. T., Smith, J. W., Ewing, G. E., & Jarrold, M. F. (2008). Charge separation in the aerodynamic breakup of micrometer-sized water droplets. *Journal of Physical Chemistry A*, *112*(December (51)), 13352–13363.
Zobnin, A. V., Nefedov, A. P., Sinel'Shchikov, V. A., & Fortov, V. E. (2000). On the charge of dust particles in a low-pressure gas discharge plasma. *Soviet Journal of Experimental and Theoretical Physics*, *91*(September), 483–487.